Fukushima ^{137}Cs releases dispersion modelling over the Pacific Ocean. Comparisons of models with water, sediment and biota data

December 14, 2018

Abstract

A number of marine radionuclide dispersion models (both Eulerian and Lagrangian) were applied to simulate ^{137}Cs releases from Fukushima Daiichi nuclear power plant accident in 2011 over the Pacific at oceanic scale. Simulations extended over two years and both direct releases into the ocean and deposition of atmospheric releases on the ocean surface were considered. Dispersion models included an embedded biological uptake model (BUM). Three types of BUMs were used: equilibrium, dynamic and allometric. Model results were compared with ^{137}Cs measurements in water (surface, intermediate and deep layers), sediment and biota (zooplankton, non-piscivorous and piscivorous fish). A reasonable agreement in model/model and model/data comparisons was obtained.

Keywords: Fukushima-Daiichi accident; dispersion model; ocean; sediment; biological uptake model; caesium

1 Introduction

After the 9.0 magnitude earthquake and resulting tsunami occurred on March 11th, 2011, in Japan, significant amounts of radioactive material were released to the environment from Fukushima Dai-ichi nuclear power plant (FDNPP). Radionuclides released to the atmosphere were transported eastward by a strong jet stream and reached the coast of North America in four days (Takemura et al., 2011). A portion of these radionuclides was deposited on the Pacific Ocean surface by wet and dry deposition processes. In addition,

water used to cool a damaged nuclear reactor leaked into the ocean (Kobayashi et al., 2013).

Some exercises comparing numerical model performances when applied to simulate the ^{137}Cs releases from FDNPP in the Pacific Ocean have been carried out, as for instance in Masumoto et al. (2012). These authors found discrepancies between the five participating models and concluded that they were due to the different calculated current fields in the coastal waters of Japan, off Fukushima, which lead to different radionuclide distributions. Differences in circulation fields were caused by the different ocean models and dispersion model settings used by the research groups. However, a systematic assessment aimed at investigating the reasons of differences was not carried out.

The Science Council of Japan (SCJ, 2014) carried out a similar intercomparison study for ^{137}Cs, with eleven models involved. Again, significant differences between models were found. Models were different in concept (Eulerian vs. Lagrangian), with different setting and even different source terms. It was concluded that a simple comparison was not straightforward and consequently detailed systematic comparison studies, such as ones that use the same radionuclide forcing with different models and/or the same model with different forcing scenarios, were required. This kind of intercomparison exercise was carried out in the frame of IAEA (International Atomic Energy Agency) MODARIA[1] program (Periáñez et al., 2015a; 2016a). The MODARIA project was running from 2012 to 2015 to make progress in the assessment of radioactive substances in the environment and its impact to man and biota. Different dispersion models were applied to simulate FDNPP releases in the Pacific, using different and also the same water circulation fields. Simulations with the same set of parameters (like diffusion coefficients for instance) were also carried out. It was found that the main source of discrepancy between different dispersion models was due to the different circulation fields. Model/model and model/measurements

[1]Modelling and Data for Radiological Impact Assessments. Further information can be found here: http://www-ns.iaea.org/projects/modaria/default.asp?l=116

comparisons for both the dissolved phase and bed sediments (not included in earlier model comparison exercises) were carried out in such study.

Alternatively, the same dispersion model forced with different circulation fields was tested as well, although water/sediment interactions were not included in this study (Kawamura et al., 2017).

An interesting exercise was described in Maderich et al. (2018). In this case the same dispersion model, running with generic parameters, was applied to describe ^{137}Cs dispersion from Chernobyl NPP accident in the Baltic and Black seas, and FDNPP accident in the Pacific Ocean. The applied box model (POSEIDON-R; Lepicard et al., 2004; Maderich et al., 2014a; 2014b; Bezhenar et al., 2016) contained an embedded food web model. Comparisons of model results with measurements in the three scenarios indicated that, with some restrictions, the model could be used with generic parameter values in radiation emergency situations in areas where limited information is available.

MODARIA-II program[2] was launched by the IAEA in 2016 as a follow-up of MODARIA. The work in comparing numerical model performances when applied to simulate FDNPP releases in the ocean was continued in the frame of this project. Nevertheless, spatial range and temporal frame of simulations were extended: two year long simulations over almost the whole North Pacific Ocean were carried out. In addition, marine dispersion models contain an integrated biological uptake model (BUM) with four components (phytoplankton, zooplankton, non-piscivorous and piscivorous fish). Model/model and model/data comparisons were carried out for water, bed sediments and biological components of the models, which has not been done before.

Six institutes have participated in the model comparisons. These are the Institute of Mathematical Machines and System Problem (IMMSP, Ukraine), Korea Institute of Ocean Science and Technology (KIOST, Rep. of Korea), ABmerit (Slovakia), University of Seville (USEV, Spain), Japan Atomic Energy Agency (JAEA, Japan), and Korea

[2]http://www-ns.iaea.org/projects/modaria/modaria2.asp?s=8&l=129

Atomic Energy Research Institute (KAERI, Rep. of Korea).

The methodology is presented in section 2, where water circulation used by models, source terms, and the origin of experimental data on ^{137}Cs concentrations are described. Results are presented in section 3. Some general discussion on model uncertainty and complexity is finally included in section 4.

2 Methods

2.1 Hydrodynamics

Water circulation provided by FORA[3] model was used for calculations. This model, Four-dimensional Variational Ocean ReAnalysis for the Western North Pacific (FORA-WNP30), is the first-ever dataset covering the western North Pacific over the last three decades (1982-2014) at eddy-resolving resolution. It is a cooperative work of the Japan Agency for Marine-Earth Science and Technology (JAMSTEC) and the Meteorological Research Institude, Japan Meteorological Agency (JMA/MRI) using the Earth Simulator (Usui et al., 2017; Tsujino et al., 2010).

The domain used in the present calculations extends 117°E-160°W and 15°N-65°N in longitude and latitude, respectively. Horizontal resolution is 0.1° and there are 54 vertical levels (0-6300 m) with increasing thickness from the surface to the sea bottom. Monthly climatological data from 2011 to 2014 were used. Two year long (March 11, 2011 to March 11, 2013) simulations were made.

The model domain showing water depths and an example of surface water circulation (averaged value for March 2011) can be seen in Fig. 1. The general large scale circulation in the western Pacific Ocean is dominated by the interaction between the Kuroshio and Oyashio currents. The Kuroshio Current is the western boundary current in the north Pacific, which flows along the coast of Japan towards the north and curves to the central

[3]http://synthesis.jamstec.go.jp/FORA/e/index.html

Pacific Ocean, then forming the so-called Kuroshio Extension. The Oyashio Current is a cold current which flows from the north. These two current systems converge in the coastal waters off Fukushima coast. Such convergence leads to the generation of unsteady eddies in the area. These features may be seen in Fig. 1.

2.2 Radionuclide sources

Radionuclides were directly introduced into the Pacific Ocean from FDNPP. They were also released to the atmosphere; radionuclides which were later deposited on the sea surface. Both sources were considered in calculations.

Direct releases of ^{137}Cs are given for the period March 25th, 2011, to December 31th, 2011, and presented in Fig. 2. They were reconstructed by JAEA as explained in detail in Kobayashi et al. (2013). Monitoring data from the web site of Tokyo Electric Power Company (TEPCO), regarding the area near the northern and southern discharge channels of the Fukushima Daiichi NPP (TEPCO, 2011), were used for this purpose.

Atmospheric deposition in the North Pacific Ocean was obtained from the averaged values from WSPEEDI-II (JAEA: Terada et al., 2012) and LADAS (KAERI: Suh et al., 2006; Suh et al., 2009) atmospheric dispersion models for the period March 12th, 2011, to June 1st, 2011. Even though simulations are 2 year long, most deposition occurred within the first months after the accident. Daily integrated values were provided. As an example, the integrated deposition for March 15th, 2011, averaged from both models, is presented in Fig. 2.

In addition, a pre-FDNPP accident ^{137}Cs uniform background of 1.5 Bq/m^3 was considered over the Pacific Ocean waters, in order to carry out comparisons of model results with field measurements.

2.3 Dispersion models

Some of the main characteristics of the dispersion models which were applied are summarized in Table 1. Both Eulerian and Lagrangian models were used with different parameterizations of horizontal and vertical diffusivities. The general characteristics and basic equations describing the two types of dispersion models which were applied are presented in appendix A.1 and A.2.

A kinetic (dynamic) approach was applied to describe water/sediment interactions in both Eulerian and Lagrangian models, which is based on a desorption coefficient and the distribution coefficient, k_d, of the corresponding radionuclide (Periáñez, 2005).

All models used an equilibrium distribution coefficient of 2.0 m^3/kg. This is the mean value recognized by IAEA (2004) for open ocean waters and is also in agreement with measurements off Fukushima (Honda et al., 2012). The kinetic rate describing release from sediments, $k_2 = 1,16 \times 10^{-5}$ s^{-1}, was determined for Cs from experiments (Nyffeler et al., 1984). The kinetic rate describing uptake (k_1) is derived from k_2 and the distribution coefficient, as usually done (Periáñez, 2005). A stochastic method is used to solve uptake/release processes in Lagrangian models (Periáñez and Elliott, 2002).

Most models include a biological uptake model (BUM). Four species were considered: phytoplankton, zooplankton, non-piscivorous and piscivorous fish. Three types of BUM were used in the models: an equilibrium model based upon a concentration factor CR (appendix B.1), a dynamic model (B.2) and an allometric method (B.3). The BUM incorporated within each physical dispersion model is indicated in Table 1 as a reference to the appendix where the corresponding BUM characteristics are commented.

2.4 Experimental data

Model results were compared with available ^{137}Cs measurements in water at three different layers, bed sediments and biological compartments (zooplankton, non-piscivorous and

Model	I/K THREETOX (IMMSP/KIOST)	I/K Lagrangian (IMMSP/KIOST)	ESTE (ABmerit)	USEV (Univ. Seville)	SEA-GEARN (JAEA)	LORAS (KAERI)
Model type	Eulerian	Lagrangian	Lagrangian	Lagrangian	Lagrangian	Lagrangian
Reference	Maderich et al. (2016)	Brovchenko et al. (2018)	www.abmerit.sk	Periáñez et al. (2016b)	Kobayashi et al. (2007)	Min et al. (2013)
Horizontal diffusion	Smagorinsky[a] formula	10 m^2/s	Smagorinsky formula	Smagorinsky formula	10 m^2/s	10 m^2/s
Vertical diffusion	10^{-4} m^2/s	10^{-3} m^2/s for $d < 60$ m 10^{-5} m^2/s for $d > 120$ m linear function for $60 < d < 120$ m	10^{-4} m^2/s	10^{-4} m^2/s	10^{-4} m^2/s	10^{-3} m^2/s
Bed porosity	0.6	0.6	0.6	0.6	0.6	0.7
Sediment thickness	0.05 m	0.05 m	0.05 m	0.05 m	0.05 m	0.1 m
Particle density	2600 kg/m^3	2600 kg/m^3	2600 kg/m^3	2600 kg/m^3		2600 kg/m^3
^{137}Cs k_d	2 m^3/kg	2 m^3/kg	2 m^3/kg	2 m^3/kg	2 m^3/kg	2 m^3/kg
k_2 (s^{-1})	3.17×10^{-8}	Maderich et al. (2017)	1.16×10^{-6}	1.16×10^{-6}	1.16×10^{-6}	1.16×10^{-6}
BUM	B.2	B.2	B.1	B.2	no	B.3

Table 1: Model main characteristics. d is water depth and k_2 is the ^{137}Cs desorption coefficient. [a] See for instance Cushman-Roisin and Beckers (2011). A selected reference is given for each model. The BUM row indicates the appendix where some details of the uptake model are given: B.1 is an equilibrium model, B.2 is a dynamic model and B.3 is the allometric method.

piscivorous fish) in the surface layer (to 20 m depth). The other two considered water layers are 20-460 m and 460 m to the seabed.

Measurements were compiled from the following references: Honda et al. (2012), Charette et al. (2013), Kaeriyama et al. (2013) for water; the "Database for Radioactive Substance Monitoring Data"[4] for sediments; Honda et al. (2012), Kitamura et al. (2013) for zooplankton; Wada et al. (2016); Men et al. (2017); Johansen et al. (2014) for fish (piscivorous and non-piscivorous). Only data for pelagic fish were used. Sampled pelagic non-piscivorous fish are *Engraulis japonicus*, *Etrumeus teres*, *Clupea pallasii* and *Hyporhamphus sajori*. Sampled pelagic piscivorous fish are *Hexagrammos sebastes*, *Todarodes pacificus*, *Snake mackerel*, *Oncorhynchus keta*, *Ammodytes japonicus*, *Seriola quinqueradiata*, *Seriola quinqueradiata*, *Trachurus japonicus* and *Scomber japonicus*. Water samples collected in the direct release area have been filtered out since the models are giving average value of radionuclide concentrations over boxes, as explained below.

Locations where samples were collected during the simulation period are indicated as dots in Fig. 3. The Pacific Ocean was divided into a number of boxes, presented in Fig. 4, according to general circulation and the location of the release point. Model results were averaged for each box and then these averaged values were compared with measurements.

Boxes in the release area may be too large for a detailed study of radionuclide behaviour in such region close to FDNPP. However, it should be taken into account that the dispersion of FDNPP ^{137}Cs releases was studied at a smaller spatio-temporal scale in a previous paper of the group (Periáñez et al., 2015a); and model predictions and measurements were compared in the area close to FDNPP (less than some 100 km away). The present work is complementing such previous paper, going to larger spatial and temporal scales. Thus, large boxes are used. In addition, it should be considered that a model/data comparison for specific points in such a large domain is not feasible with Lagrangian models which release individual particles, and it is better to use averages over

[4]http://emdb.jaea.go.jp/emdb/en/

given areas, which are defined in view of the physical oceanography of the region (Periáñez et al., 2015a; 2015b; 2016a). However, it should be noted that measurements were not distributed homogeneously in the relatively large considered boxes.

3 Results

As explained before, two year long simulations were carried out; from March 2011 to March 2014. Monthly mean values of ^{137}Cs concentrations in each box in Fig 4 were provided by the models for the three water layers, seabed sediments and the four biological compartments (surface layer only).

Model results and ^{137}Cs measurements are presented in Fig. 5 to Fig. 12. Results are presented only for such boxes where measurements are available. Results for the abiotic and biotic components of the models are discussed separately in the following subsections.

3.1 Water and sediments

Results for surface water may be seen in Fig. 5 and Fig. 6, for boxes which are far from Japan and boxes located closer, around FDNPP, respectively. In boxes 1, 3, 5 and 20 (Fig. 5) there is a slight increase in ^{137}Cs concentrations with respect to background immediately after the accident, which must be attributed to atmospheric deposition. In general, models produce this initial increase, which is about one order of magnitude above background. In other boxes (like 15 and 16), both models and measurements indicate pre-FDNPP accident background. Thus, releases did not affect these areas in the considered temporal frame.

In contrast, high concentrations are found closer to FDNPP (Fig. 6). For some of the boxes (6, 7, 12) models and measurements show a trend towards achieving background concentrations after approximately one year. The initial concentration increase above background is about two orders of magnitude. Other regions south from Japan (boxes 13

and 14) do not seem to be affected by FDNPP releases, although some models predict a slight concentration increase above background. Direct releases from FDNPP into the ocean occur in box 11; consequently very high ^{137}Cs concentrations were measured here, especially soon after the accident. Although samples collected just in the release area are not considered, as commented above, obviously there must be a significant underestimation of ^{137}Cs concentrations in this box in the period of acute discharges. This can be clearly seen in Fig. 7, where the geometric means of measured concentrations in boxes 10 and 11 for each month are represented together with box averaged model predictions. Mean values of measured concentrations in both boxes decrease in up to three orders of magnitude. While all models underestimate measurements in the early period after the accident, the mean values of measurements are within the range of model predictions after such initial phase.

Generally speaking, models agree in predicting areas in the Pacific Ocean which were affected by FDNPP releases (direct and/or atmospheric deposition) and regions which were not. In addition, there is a relatively good agreement between the temporal trends of ^{137}Cs concentrations predicted by the different models. In most cases, concentrations are within the same order of magnitude.

Results for intermediate and deep waters are presented in Fig. 8. In these cases measurements were not carried out soon after the accident. Models indicate an increase in ^{137}Cs concentrations (about a factor 10^2) immediately after FDNPP accident and a decrease to background concentrations for intermediate waters. Both models and measurements show concentrations in the deep later of the same order of magnitude as background. Thus, deep water in these regions (boxes 10 and 11) was not affected by the accident in the considered temporal frame. Again, there is a relatively good agreement between outputs of the different models.

The case of sediments may be seen in Fig. 9. ^{137}Cs concentration in the bed sediment increase significantly over background in boxes 10 and 11, which are the closer to FDNPP

than box 9. Models predict such increase, although with larger discrepancy between models than in the case of the dissolved phase. In contrast, background levels are apparent in box 9, north from the previous ones. It is interesting to note that a decreasing trend of ^{137}Cs concentrations in sediments close to FDNPP (less than some 100 km away) has been observed (Kusakabe et al., 2013) after the period of acute releases. Sediments at larger distances from FDNPP do not show such decreasing trend (dots in Fig. 9, box 10 and 11). Thus, it seems that these sediments are buffering radionuclides. Most models also predict quite constant ^{137}Cs concentrations in these sediments and the range of model predictions is within the range of measured concentrations. The geometric means of measured concentrations in boxes 10 and 11 for each month are represented together with box averaged model predictions in Fig. 7. Mean values of measured concentrations in sediments in both boxes effectively do not show any clear decreasing trend; and these mean values of measurements are within the range of model predictions, as mentioned above.

3.2 Biotic components

Results for zooplankton are presented in Fig. 10 for boxes were measurements are available. Model results are in general within the same order of magnitude. However, most models significantly underestimate measured concentrations. Zooplankton takes ^{137}Cs from phytoplankton (which in dynamic models is in equilibrium with water [see appendix B.2]) and directly from water as well. Thus, there are not significant differences in the temporal trends produced for zooplankton by equilibrium and dynamic models. The allometric approach (LORAS model) leads to larger concentrations in boxes 7 and 12, which are in better agreement with observations then the other models. The better agreement of LORAS model with measurements for zooplankton (and further for fish) can be explained by the higher concentration in water predicted by this model.

Non zero concentrations in biota calculated by USEV model before FDNPP accident are due to the fact that background concentrations are assumed in water since $t = 0$, that in this model is January 1st. Thus, biotic components of the model absorb such background ^{137}Cs.

Results for non-piscivorous and piscivorous fish are respectively shown in Figs. 11 and 12. Now differences between equilibrium and dynamic models become clearer. ^{137}Cs concentrations predicted by an equilibrium model reflect concentrations in water. Thus, peak values are reached simultaneously in water and fish. There is a delay in the time of peak fish concentrations with respect to peak concentrations in water in the case of dynamic models. This different behaviour of equilibrium and dynamic models was already pointed out in the BUM intercomparison carried out by Vives i Battle et al. (2016) in the frame of IAEA MODARIA program. However, in such exercise BUMs were not included within full marine dispersion models. Instead, BUM model responses were tested in a single point where ^{137}Cs concentration in water was prescribed (what could be denoted as a zero-dimensional model).

Both models including a dynamic BUM (THREETOX and USEV) produce similar outputs in spite of being models with different structure (Eulerian and Lagrangian respectively). Both models use the same generic parameters described in Maderich et al. (2014a). Thus, these results are supporting the findings in Maderich et al. (2018): this BUM model is robust enough to be used with generic parameters in areas where limited information is available. Concentration levels produced by the equilibrium model in fish are, in general, in better agreement with measurements than calculations by dynamic models and allometry. This is due to the higher concentrations that ESTE model (which uses the equilibrium approach) produces in water (Fig. 6) and should not be attributed to the BUM itself. Nevertheless, the instantaneous equilibrium with activity concentration in seawater does not seem to be realistic (Vives i Battle et al., 2016).

The allometric model output generally is more similar to the dynamic models in the

case of non-piscivorous fish and to the equilibrium model in the case of piscivorous fish. However there are not enough experimental data to assess which model produces a more realistic behaviour.

4 Discussion

In a previous work (Periáñez et al., 2015a) it was found that the main source of discrepancy between dispersion models is water circulation. Discrepancy between models is significantly reduced if the same water circulation fields are used by all dispersion models. However, other sources of uncertainty in model/model comparisons exist. This uncertainty is due to model parameters and model numerics.

If the model is applied to a perfectly conservative radionuclide (remaining dissolved, without any interactions with sediments) the only involved parameters are the horizontal and vertical diffusion coefficients. Turbulence is an open problem in physics and has to be parameterized. Thus, different schemes and approaches are used to evaluate diffusion coefficients. These different approaches may lead to different model results. The situation is even more complex for non-conservative radionuclides. A number of parameters is required in this case, like kinetic rates, particle sizes, density and thickness of the sediment, etc. These parameters are site-specific and information about them is generally scarce. Thus, only realistic or tentative values have often to be used. Dynamic models need more parameters in comparison with more simple approaches based on sediment distribution coefficients and concentration ratios for biota, but they are less site-dependent.

The second source of uncertainty is due to model numerics. A numerical solution always requires discretization in time. A spatial discretization is required in Eulerian models. However, even in Lagrangian models a spatial discretization is required when concentrations are derived from the number of particles per water volume unit, resulting in averaging of quantities. A discretization always implies averaging magnitudes; and

averaging leads to errors. Moreover, a numerical solution is only an approximation to the exact solution since several errors appear (rounding errors, truncation errors etc). The radionuclide release area size has to be considered as well. In Eulerian models, radionuclides are homogeneously distributed into the release cell where the accident occurs; this would be the initial patch minimum size. Thus, the initial patch size depends on the model spatial resolution. This initial patch size defines the initial peak concentration. In contrast, a real point source can be used in a Lagrangian model. Obviously, this will lead to differences between Eulerian and Lagrangian models.

It is essential to have accurate oceanographic data to compare model results with measurements. However, it is hard to obtain accurate predictions of water currents in energetic regions characterized by strong current variability, like Fukushima waters and the North Western Pacific region, which are characterized by the very strong and fluctuating Kuroshio current ant its extension (Masumoto et al., 2012). Different hydrodynamic models will lead to slightly different current fields. Given the intensity and variability of currents in these energetic areas, as well as the presence of unsteady eddies, small differences in the hydrodynamics may produce differences in dispersion patterns which tend to be amplified with time.

Another issue is how to chose the most appropriate level of model complexity for a given problem. Of course, this is related to the expected end-point of a simulation. This will define the spatio-temporal resolving power of the model (Monte et al., 2006), which is a measure of the level of detail of its predictions. The time resolving power is the ability of a model to predict differences in the system behaviour over a given interval of time. Similarly, the spatial resolving power is the ability of a model to predict differences in the system behaviour over a given spatial grid. Of course, model complexity increases with the resolving power.

Models with different complexities have been used in the present paper to calculate radionuclide concentrations in biota (from equilibrium to dynamic models). As stated in

Monte et al. (2006), the general principle that the simplest model is ever better than the complex one, if they supply similar results for some given particular applications, should be avoided. A simple model may not be sufficiently developed for application to the innumerable possible contamination scenarios, marine systems and environmental circumstances that other more complex and general models are meant to simulate. For instance, as has been commented above, peak ^{137}Cs concentrations are reached simultaneously in water and fish if an equilibrium model is used. On the other hand, there is a delay in the time of peak fish concentrations with respect to peak concentrations in water in the case of dynamic models; which is more realistic. Thus, the simple (equilibrium) model is not suitable for the study of the initial phase of an accident. A more complex model, able to deal with non-equilibrium situations, should be applied for this purpose.

5 Conclusions

A number of physical dispersion models of different natures (Eulerian and Lagrangian) were applied to simulate FDNPP ^{137}Cs releases in the Pacific Ocean over two years and at oceanic scale. Realistic source terms for direct releases and atmospheric deposition were used. Most models included a biological uptake model consisting of four species: phytoplankton, zooplankton, non-piscivorous and piscivorous fish. There types of biological uptake models were tested: equilibrium model, dynamic model and an allometry method. Model results were compared with measurements in water (three layers), sediment and biota.

In general, there is a good agreement between models and between models and measurements. The method used to compare models is helping in this regards. It was found (Periáñez et al., 2015a) that comparisons of Lagrangian model outputs in specific points is difficult since a number of discrete particles are released in these models. Thus, it is more convenient to divide the oceanic space into a number of boxes and to obtain average

concentrations over such boxes; as it was done for the Baltic Sea model intercomparison in Periáñez et al. (2015b). However, it should be taken in account that in the vicinity of FDNPP measurements were not distributed homogeneously in space. This can result in overestimation of experimental box-averaged values.

Models agree in predicting areas in the Pacific Ocean which were affected by FDNPP releases (direct and/or atmospheric deposition) and regions which were not. In addition, predicted concentrations are within the same order of magnitude in most cases.

With respect to calculated ^{137}Cs temporal trends in biota, dynamic models tend to underestimate concentrations. Allometry and the equilibrium approach results are, in general, in better agreement with observations. This is explained by the higher ^{137}Cs concentrations in water produced by ESTE and LORAS models. Temporal evolutions of ^{137}Cs concentrations calculated through the different approaches are different, although there is not enough experimental data to assess which approach leads to better results. However, it is clear that dynamic models provide the known pattern of delayed rise of activity concentration in biota.

Acknowledgement

Work carried out in the frame of IAEA MODARIA-II (Modelling and Data for Radiological Impact Assessments) program. This work was partially supported by the National Research Foundation of Korea (NRF) and partially funded by the Korean Government (MSIP) (MSIP: NRF-2017M2A8A4015253, NRF-2015M2A2B2034282). The authors are indebted to all members of MODARIA-II working group 7 for useful discussions held during group meetings.

6 References

Bezhenar, R., Jung, K.T., Maderich, V., Willemsen, S., de With, G., Qiao, F., 2016. Transfer of radiocesium from contaminated bottom sediments to marine organisms through benthic food chain in post-Fukushima and post-Chernobyl periods. Biogeosciences 13, 3021-3034.

Brovchenko, I., Jung, K.T., Maderich, V., Kim, K.O., Kovalets, S., 2018. Method of moments for random walk algorithms. In preparation.

Brown, J., Borrentzen, P., Dowdall, M., Sazykina, T., Kryshev, I., 2004. The Derivation of Transfer Parameters in the Assessment of Radiological Impacts on Arctic marine Biota. ARCTIC 57(3), 279-289.

Carvalho, F. P., 2018. Radionuclide concentration processes in marine organisms: A comprehensive review. Journal of Environmental Radioactivity 186, 124-130.

Charette, A.M. Breier, C.F., Henderson, P.B., Pike, S.M., Rypina,I.I., Jayne, S.R., Buesseler, K.O., 2013. Radium-based estimates of cesium isotope transport and total direct ocean discharges from the Fukushima Nuclear Power Plant accident, Biogeosciences 10, 2159-2167.

Cushman-Roisin, B., Beckers, J.M., 2011. *Introduction to Geophysical Fluid Dynamics*. Elsevier.

Heling, R., Koziy, L., Bulgakov, V., 2002. On the dynamical uptake model developed for the uptake of radionuclides in marine organisms for the POSEIDON-R model system. Radioprotection 37(C1), 833-838.

Higley, K.A., Domotor, S.L., Antonio, E.J., Kocher, D.C., 2003. Derivation of a screening methodology for evaluating radiation dose to aquatic and terrestrial biota. Journal of Environmental Radioactivity, 66, 41-59.

401 Honda M., Aono T., Aoyama M., Hamajima Y., Kawakami H., Kitamura M., Ma-
402 sumoto Y., Miyazawa Y., Takigawa M., Saino T., 2012. Dispersion of artificial
403 caesium-134 and -137 in the western North Pacific one month after the Fukushima
404 accident. Geochemical Journal 46, 1-9.

405 IAEA, 2004. Sediment distribution coefficients and concentration factors for biota
406 in the marine environment. Technical Reports Series 422, Vienna.

407 Johansen, M.P., Ruedig, E., Tagami, K., Uchida, S., Higley, K., Beresford, N., 2014.
408 Radiological dose rates to marine fish from the Fukushima Daiichi accident: the first
409 three years across the North Pacific, Environmental Science and Technology 49(3),
410 1277-1285.

411 Kaeriyama, H., Ambe, D., Shimizu, Y., Fujimoto, K., Ono, T., Yonezaki, S., Kato,
412 Y., Matsunaga, H., Minami, H., Nakatsuka, S., Watanabe, T., 2013. Direct ob-
413 servation of ^{134}Cs and ^{137}Cs in surface seawater in the western and central North
414 Pacific after the Fukushima Dai-ichi nuclear power plant accident, Biogeosciences
415 10, 4287-4295.

416 Kawamura, H., Furuno, A., Kobayashi, T., In, T., Nakayama, T., Ishikawa, Y.,
417 Miyazawa, Y., Usui, N., 2017. Oceanic dispersion of Fukushima-derived Cs-137
418 simulated by multiple oceanic general circulation models. Journal of Environmental
419 Radioactivity 180, 36-58.

420 Kitamura, M., Kumamoto, Y., Kawakami, H., Cruz, E.C., Fujikura, K., 2013. Hor-
421 izontal distribution of Fukushima-derived radiocesium in zooplankton in the north-
422 western Pacific Ocean. Biogeosciences 10, 5729-5738.

423 Kobayashi, T., Otosaka, S., Togawa, O., Hayashi, K., 2007. Development of a
424 nonconservative radionuclides dispersion model in the ocean and its application

425 to surface cesium-137 dispersion in the Irish Sea. Journal of Nuclear Science and
426 Technology 44(2), 238-247.

427 Kobayashi, T., Nagai, H., Chino, M., Kawamura, H., 2013. Source term estimation
428 of atmospheric release due to the Fukushima Dai-ichi Nuclear Power Plant accident
429 by atmospheric and oceanic dispersion simulations. Journal of Nuclear Science and
430 Technology 50, 255-264.

431 Kusakabe, M., Oikawa, S., Takata, H., Misonoo, J., 2013. Spatiotemporal dis-
432 tributions of Fukushima-derived radionuclides in nearby marine surface sediments.
433 Biogeosciences 10, 5019-5030.

434 Lepicard S., Heling R., Maderich V. 2004. POSEIDON/RODOS model for radio-
435 logical assessment of marine environment after accidental releases: application to
436 coastal areas of the Baltic, Black and North seas. Journal of Environmental Ra-
437 dioactivity 72, 1-2, 153-161

438 Lynch D.R., Greenberg D.A., Bilgili A., Mcgillicuddy, D.J., Manning, J.P., Aretx-
439 abaleta A.L., 2015. Particles in the Coastal Ocean. Theory and Applications.
440 Cambridge University Press, NY.

441 Maderich V., Heling R., Bezhenar R., Brovchenko I., Jenner H., Koshebutskyy V.,
442 Kuschan A., Terletska K.. 2008. Development and application of 3D numerical
443 model THREETOX to the prediction of cooling water transport and mixing in the
444 inland and coastal waters. Hydrological Processes 22, 1000-1013.

445 Maderich, V., Bezhenar, R., Heling, R., de With, G., Jung, K.T., Myoung, J.G.,
446 Cho, Y.K., Qiao, F., Robertson, L., 2014a. Regional long-term model of radioac-
447 tivity dispersion and fate in the northwestern Pacific and adjacent seas: application
448 to the Fukushima Dai-ichi accident. Journal of Environmental Radioactivity 131,
449 4-18.

Maderich V., Jung, K.T., Bezhenar R., de With, G., Qiao F., Casacuberta, N., Masqué, P., Kim, Y.H., 2014b. Dispersion and fate of ^{90}Sr in the Northwestern Pacific and adjacent seas: Global fallout and the Fukushima Dai-ichi accident. Science of the total Environment 494-495, 261-271.

Maderich V., Brovchenko I., Dvorzhak A., Ievdin I., Koshebutsky, V., Periañez, R., 2016. Integration of 3D model THREETOX in JRODOS, implementation studies and modelling of Fukushima scenarios. Radioprotection 51(HS2), S133-S135.

Maderich, V., Jung, K.T., Brovchenko, I., Kim, K.O., 2017. Migration of radioactivity in multi-fraction sediments. Environmental Fluid Mechanics 17, 1207-1231.

Maderich, V., Bezhenar, R., Tateda, Y., Aoyama, M., Tsumune, D., 2018. Similarities and differences of ^{137}Cs distributions in the marine environments of the Baltic and Black seas and off the Fukushima Dai-ichi nuclear power plant in model assessments. Marine Pollution Bulletin 135, 895-906.

Masumoto, Y., Miyazawa, Y., Tsumune, D., Kobayashi, T., Estournel, C., Marsaleix, P., Lanerolle, L., Mehra, A., and Garraffo, Z.D., 2012. Oceanic dispersion simulation of Cesium-137 from Fukushima Dai-ichi nuclear power plant, Elements, 8, 207-212.

Men, W., Deng, F., He, J., Yu, W., Wang, F., Li, Y., Lin, F., Lin, J., Lin, L., Zhang, Y., Yu, X., 2017. Radioactive impacts on nekton species in the Northwest Pacific and humans more than one year after the Fukushima nuclear accident, Ecotoxicology and Environmental Safety 144, 601-610.

Min, B.I., Periáñez, R., In-Gyu Kim, Kyung-Suk Suh, 2013. Marine dispersion assessment of ^{137}Cs released from the Fukushima nuclear accident. Marine Pollution Bulletin 72, 22-33.

Monte, L., Hakason, L., Periáñez,R., Laptev, G., Zheleznyak, M., Maderich, V.,

474 Koshebutsky, V., 2006. Experiences from a case study of multi-model application to
475 assess the behaviour of pollutants in the Dnieper-Bug estuary. Ecological Modelling
476 195, 247-263.

477 Nyffeler, U.P., Li, Y.H., Santschi, P.H., 1984. A kinetic approach to describe
478 trace element distribution between particles and solution in natural aquatic sys-
479 tems. Geochimica Cosmochimica Acta 48, 1513-1522.

480 Periáñez, R., Elliott, A. J., 2002. A particle-tracking method for simulating the
481 dispersion of non-conservative radionuclides in coastal waters. Journal of Environ-
482 mental Radioactivity 58(1), 13-33.

483 Periáñez, R., 2005. Modelling the dispersion of radionuclides in the marine environ-
484 ment: an introduction. Springer, Berlin.

485 Periáñez, R., Bezhenar, R., Byung-Il, Min, Duffa, C., Jung, K., Kobayashi, T.,
486 Kyung-Suk, Suh, Lamego, F., Maderich,V., Nies,H., Osvath, I., Psaltaki, M., 2015a.
487 A new comparison of marine dispersion model performances for Fukushima releases
488 in the frame of IAEA MODARIA program. Journal of Environmental Radioactivity
489 150, 247-269.

490 Periáñez, R. Bezhenar, R., Iosjpe, M., Maderich, V., Nies, H., Osvath, I., Outola, I.,
491 de With, G., 2015b. A comparison of marine radionuclide dispersion models for the
492 Baltic Sea in the frame of IAEA MODARIA program. Journal of Environmental
493 Radioactivity 139, 66-77.

494 Periáñez, R., R. Bezhenar, I. Brovchenko, C. Duffa, K.T. Jung, T. Kobayashi, F.
495 Lamego, V. Maderich, B.I. Min, H. Nies, I. Osvath, I. Outola, M. Psaltaki, K.S.
496 Suh, G. de With, 2016a. Modelling of marine radionuclide dispersion in IAEA
497 MODARIA program: lessons learnt from the Baltic Sea and Fukushima scenarios.
498 Science of the Total Environment 569/570, 594-602.

499 Periáñez, R., Kyung-Suk Suh, Byung-Il Min, 2016b. The behaviour of ^{137}Cs in the
500 North Atlantic Ocean assessed from numerical modelling: releases from nuclear fuel
501 reprocessing factories, redissolution from contaminated sediments and leakage from
502 dumped nuclear wastes. Marine Pollution Bulletin 113, 343-361.

503 Proehl, J.A., Lynch, D.R., McGuillicuddy, D.J., Ledwell, J.R., 2005. Modeling
504 turbulent dispersion on the North Flank of Georges Bank using Lagrangian particle
505 methods. Continental Shelf Research 25, 875-900.

506 Protter, P.E., 2004. Stochastic Integration and Differential Equations (2nd ed.).
507 Springer, ISBN 3-540-00313-4.

508 Schmidt-Nielsen, K., 1977. Problems of scaling: locomotion and physiological cor-
509 relates. In: *Scale Effects in Animal Locomotion*, T.J. Pedley (editor). Academic
510 Press, New York. pp. 1-21.

511 SCJ, 2014. A review of the model comparison of transportation and deposition of
512 radioactive materials released to the environment as a result of the Tokyo Electric
513 Power Compny's Fukushima Daiichi Nuclear Power Plant accident. Report of the
514 Sectional Committee on Nuclear Accident Committee on Comprehensive Synthetic
515 Engineering, Science Council of Japan.

516 Suh, K.S., Jeong, H.J., Kim, E.H., Hwang, W.T., Han, M.H., 2006. Verification
517 of the Lagrangian particle model using the ETEX experiment. Annals of Nuclear
518 Energy 33, 1159-1163.

519 Suh, K.S., Han, M.H., Jung, S.H., Lee, C.W., 2009. Numerical simulation for a long-
520 range dispersion of a pollutant using Chernobyl data. Mathematical and Computer
521 Modeling 49, 337-343.

522 Takemura, T., Nakamura, H., Takigawa, M., Kondo, H., Satomura. T., Miyasaka,

523 T., Nakajima, T., 2011. A numerical simulation of global transport of atmospheric
524 particles emitted from the Fukushima Daiichi Nuclear Power Plant. SOLA 7, 101-
525 104.

526 TEPCO, 2011. http://www.tepco.co.jp/en/nu/fukushima-np/f1/index2-e.html.

527 Terada, H., Katata, G., Chino, M., Nagai, H., 2012. Atmospheric discharge and
528 dispersion of radionuclides during the Fukushima Dai-ichi Nuclear Power Plant ac-
529 cident. Part II: verification of the source term and analysis of regional-scale atmo-
530 spheric dispersion. Journal of Environmental Radioactivity 112, 141-154.

531 Tsujino, H., Motoi, T., Ishikawa, I., Hirabata, M., Nakano, H., Yamanaka, G.,
532 Yasuda, T., Ishizaki, H., 2010. Reference Manual for the Meteorological Research
533 Institute Community Ocean Model (MRI.COM) Version 3. Tsukuba (Japan): Me-
534 teorological Research Institute. Technical Reports of the MRI, 59.

535 Usui, N., Wakamatsu, T., Tanaka, Y., Hirose, N., Toyoda, T., Nishikawa, S., Fujii,
536 Y., Takatsuki, Y., Igarashi, H., Ishikawa, Y., Kuragano, T., Kamachi, M., 2017.
537 Four-dimensional Variational Ocean Reanalysis: A 30-year high-resolution dataset
538 in the western North Pacific (FORA-WNP30). Journal of Oceanography 73(2),
539 205-233.

540 Vives i Batlle, J., Wilson, R.C., Watts, S.J., Jones, S.R., McDonald, P., Vives-
541 Lynch, S., 2008. Dynamic model for the assessment of radiological exposure to
542 marine biota, Journal of Environmental Radioactivity 99, 1711-1730.

543 Vives i Batlle, J., Beresford, N., Beaugelin-Seiller, K., Bezhenar, R., Brown, J., Jing-
544 Jy Cheng, Cujic, M., Dragovic, S.S., Duffa, C., Fievet, B., Hosseini, A., Jung, K.T.,
545 Kamboj, S., Dong-Kwon Keum, Kobayashi, T., Kryshev, A., Le Poire, D., Maderich,
546 V., Byung Il Min, Periáñez, R., Sazykina, T., Suh, K.S., Yu, C., Wang, C., Heling,

R., 2016. Inter-comparison of dynamic models for radionuclide transfer to marine biota in a Fukushima accident scenario. Journal of Environmental Radioactivity 153, 31-50.

Wada, T., Fujita, T., Nemoto, Y., Shimamura, S., Mizuno, T., Sohtome, T., Kamiyama, K., Narita, K., Watanabe, M., Hatta, N., Ogata, Y., Morita, T., Igarashi, S., 2016. Effects of the nuclear disaster on marine products in Fukushima: An update after five years. Journal of Environmental Radioactivity 164, 312-324.

West G.B,, Brown, J.H., Enquist, B.J., 1997. A general model for the origin of allometric scaling laws in biology. Science 276, 122-126.

A Physical dispersion models

Physical dispersion models (both Eulerian and Lagrangian) are based on the same general principles and equations; and then particularized as presented in Table 1. Thus, those common general descriptions are given below.

A.1 Eulerian models

In Eulerian models the differential equations giving temporal and spatial evolution of the radionuclide concentrations in different states (e.g. dissolved in water column and pore water in sediments, fixed on the suspended and bottom sediment etc) are solved. The general compact form of these equations for concentration of radioactivity C_α in state α per unit of volume (Bq m^{-3}) or per unit of mass (Bq kg^{-1}) are written in Cartesian coordinates as:

$$\frac{\partial C_\alpha}{\partial t} + \frac{\partial (u_\alpha C_\alpha)}{\partial x} + \frac{\partial (v_\alpha C_\alpha)}{\partial y} + \frac{\partial (w_\alpha C_\alpha)}{\partial z} = \frac{\partial}{\partial x}\left(K_h \frac{\partial C_\alpha}{\partial x}\right) + \frac{\partial}{\partial y}\left(K_h \frac{\partial C_\alpha}{\partial y}\right) +$$

$$+\frac{\partial}{\partial z}\left(K_v\frac{\partial C_\alpha}{\partial z}\right)+\sum_{\beta=1}^{n}k_{\beta\alpha}C_\beta+S_\alpha-\lambda C_\alpha \qquad (1)$$

where (x, y, z) are Cartesian coordinates, u_α, v_α and w_α are components of flow field for the radionuclide in the state α. In general, velocity can differ for different states (e.g. due the presence of settling velocity for suspended sediment or to be zero in the bottom deposit). K_h and K_v are turbulent or molecular diffusivities in the horizontal and vertical directions respectively, and/or biodiffusivity in the bottom deposit, which are variable in time and space. The term $\sum_{\beta=1}^{n} k_{\beta\alpha}C_\beta$ describes first order reactions between the radionuclides in different states, $k_{\beta\alpha}$ are kinetic transfer coefficients and $k_{\alpha\alpha} = -\sum_{\beta=1}^{n} k_{\alpha\beta}$ for $\alpha \neq \beta$; S_α is the radionuclide source term and λ is the radionuclide decay constant. Equations for the water column and bottom sediment layer are linked by fluxes of activity.

A.2 Lagrangian models

In Lagrangian models the released activity is represented by a number of particles, each one equivalent to a given amount of activity (Bq). The path followed by each particle is calculated and radionuclide concentrations are obtained from the number of particles per volume or mass unit. The equations describing variations of particle (in state α) position over each time increment dt are given by the Itô (Protter, 2004) stochastic differential equations:

$$dx = u_\alpha dt + \frac{\partial K_h}{\partial x}dt + \sqrt{2K_h}dW_x, \qquad (2)$$

$$dy = v_\alpha dt + \frac{\partial K_h}{\partial y}dt + \sqrt{2K_h}dW_y, \qquad (3)$$

$$dz = w_\alpha dt + \frac{\partial K_v}{\partial z}dt + \sqrt{2K_v}dW_z, \qquad (4)$$

where u_α, v_α and w_α are velocity components on coordinate axis (x, y, z) for state α; W_x, W_y, W_z are independent components of the stochastic motion (the Wiener process).

They have zero mean and variance dt ($\overline{dW_x^2} = \overline{dW_y^2} = \overline{dW_z^2} = dt$). For the finite time step Δt Wiener increments can be simulated as $\Delta W_x = \sqrt{\Delta t} R_x$, $\Delta W_y = \sqrt{\Delta t} R_y$, $\Delta W_z = \sqrt{\Delta t} R_z$, where (R_x, R_y, R_z) are normally distributed random variables having zero mean and standard deviation one. Derivatives of the diffusion coefficients above prevent the artificial accumulation of particles in regions of low diffusivity (Proehl et al., 2005; Lynch et al., 2015).

An stochastic method is used to solve the exchanges of radionuclides between the liquid and solid phases in a dynamic way. These processes are formulated using kinetic transfer coefficients, considering that exchanges of radionuclides between phases are governed by a first-order reversible reaction. Detail may be seen in Periáñez and Elliott (2002).

B Biological uptake models

Three types of biological uptake models have been applied. An equilibrium model based on concentration ratios, a dynamic model and an allometry method. They are briefly described below.

B.1 Equilibrium model

The equilibrium approximation is based on a concentration factor, CR, between water and biota. This CR, in analogy with the water/sediment k_d, is defined as the ratio between radionuclide concentration in a given specie of biota and concentration in water:

$$CR = \frac{C_{bio}}{C_w}. \tag{5}$$

Thus, concentration in biota, C_{bio}, can be calculated from the CR and the calculated concentration in water, assuming equilibrium (Carvalho, 2018). Concentration factors are determined for fishes, mollusks, crustaceans, plankton and algae, and for a large number of

elements (IAEA, 2004). These generic values have been used. In the equilibrium approach, used by ESTE model, non-piscivorous and piscivorous fish are not distinguished. Thus, results for both types of fish are supposed to be the same.

B.2 Dynamic model

The dynamic model consists of four species (Heling et al., 2002; Maderich et al., 2014a; 2014b): phytoplankton, zooplankton, non-piscivorous and piscivorous fish (Fig. 13, from Maderich et al., 2014a). The basic equation connecting concentration of activity in predator C_{pred} (Bq kg^{-1} wet weight) with activity concentration in food C_f (Bq kg^{-1} wet weight) is:

$$\frac{\partial C_{pred}}{\partial t} = aK_1C_f + bK_wC_w - K_{0.5}C_{pred}, \tag{6}$$

where K_1 (s^{-1}) is food uptake rate, a is the transfer coefficient through food, K_w is water uptake rate (s^{-1}), b is the transfer coefficient from water and C_w is activity concentration in water (Bq m^{-3}). $K_{0.5}$ is the radionuclide elimination rate from the body of fish given by $K_{0.5} = \ln 2T_{0.5}^{-1}$, where $T_{0.5}$ is the biological half-life of the radionuclide (s). Thus, all organisms take radionuclides from water, phytoplankton is the food for zooplankton, zooplankton is the food for non-piscivorous fish and this is the food for piscivorous fish (as summarized in Fig. 13). Phytoplankton exchanges radionuclides only with the water via adsorption and desorption processes. Due to the rapid uptake and short retention time of radioactivity, the concentration of radionuclides in phytoplankton is calculated using the equilibrium approach (equation 5):

$$C_{phyto} = CR_{phyto}C_w, \tag{7}$$

where CR_{phyto} (m^{3}kg^{-1}, wet weight) is the concentration ratio for phytoplankton.

Standard literature values for all these parameters for the four considered species may

	Zooplankton	Non-pisc. fish	Pisc. fish
$T_{0.5}$ (day)	5	75	200
a	0.2	0.5	0.7
b	0.001	0.001	0.001
K_1 (day^{-1})	1.0	0.035	0.0055
K_w (m^3/kg day)	1.5	0.1	0.075

Table 2: Parameters used in the dynamic BUM (from Maderich et al., 2014a). The concentration factor for phytoplankton is $CR_{phyto} = 20$ l/kg.

be seen in Maderich et al. (2014a), which have been used in calculations. They are provided in Table 2.

B.3 Allometry method

An allometric method (Schmidt-Nielsen, 1977; West et al., 1997) may be used to simulate the radionuclide concentrations in marine biota. There is a variety of marine biota, with different sizes and shapes, in the oceans. Regardless of the variety of marine species, physical correlations between individual characteristics and masses have been provided. There are several allometric equations related to many biological characters including daily food ingestion rate, water intake rate and biological half-life of radionuclides. A first-order kinetics is used to predict radionuclide concentrations in marine biota based on an allometric equation (Schmidt-Nielsen, 1977; West et al., 1997). The general form of equation is as follows:

$$q = \frac{R}{k}\left(1 - e^{-kt}\right) \tag{8}$$

where q is the total activity (Bq) in the organism of concern at time t, R is activity intake rate (Bq/day) into the organism, k is the effective loss rate of activity (1/day) from the organism, and t is the total length of exposure to the contaminant (day). Whole-body radionuclide concentration (Bq/kg) in the organism is calculated as q divided by the mass

643 M (kg):

$$C_{biota} = \frac{R}{kM}\left(1 - e^{-kt}\right) \tag{9}$$

644 where C_{biota} is the radionuclide concentration in marine biota (Bq/kg). k can be expressed
645 as follows:

$$k = \frac{\ln 2}{T_{1/2}} \tag{10}$$

646 The biological half-life of Cs for fish is (Higley et al., 2003):

$$T_{1/2} = 3.5 \times (1000 \times M)^{0.24} \tag{11}$$

647 In the case of phytoplankton and zooplankton constant values are used (Vives i Batlle et
648 al., 2008; Table 1).

649 The activity intake rate is calculated as:

$$R = A_E F_I C_f + W_I C_w - E_R C_{biota} \tag{12}$$

650 where A_E is assimilation efficiency, F_I is food intake rate, C_f is ^{137}Cs concentration in
651 food, W_I is water intake rate and E_R is excretion rate (Brown et al., 2004; tables 5 and
652 6).

653 Values for mass M of phytoplankton and zooplankton are taken from Vives i Batlle
654 et al. (2008). For non-piscivorous and piscivorous fish they are respectively assumed as
655 0.2 kg and 2 kg.

656 The semi-dynamic allometric method was applied to calculate radionuclide concen-
657 trations in marine biota from radionuclide concentrations in seawater in LORAS model.
658 This approach is a very efficient method, requiring short computational times (about one
659 minute for a two year simulation in a Linux cluster).

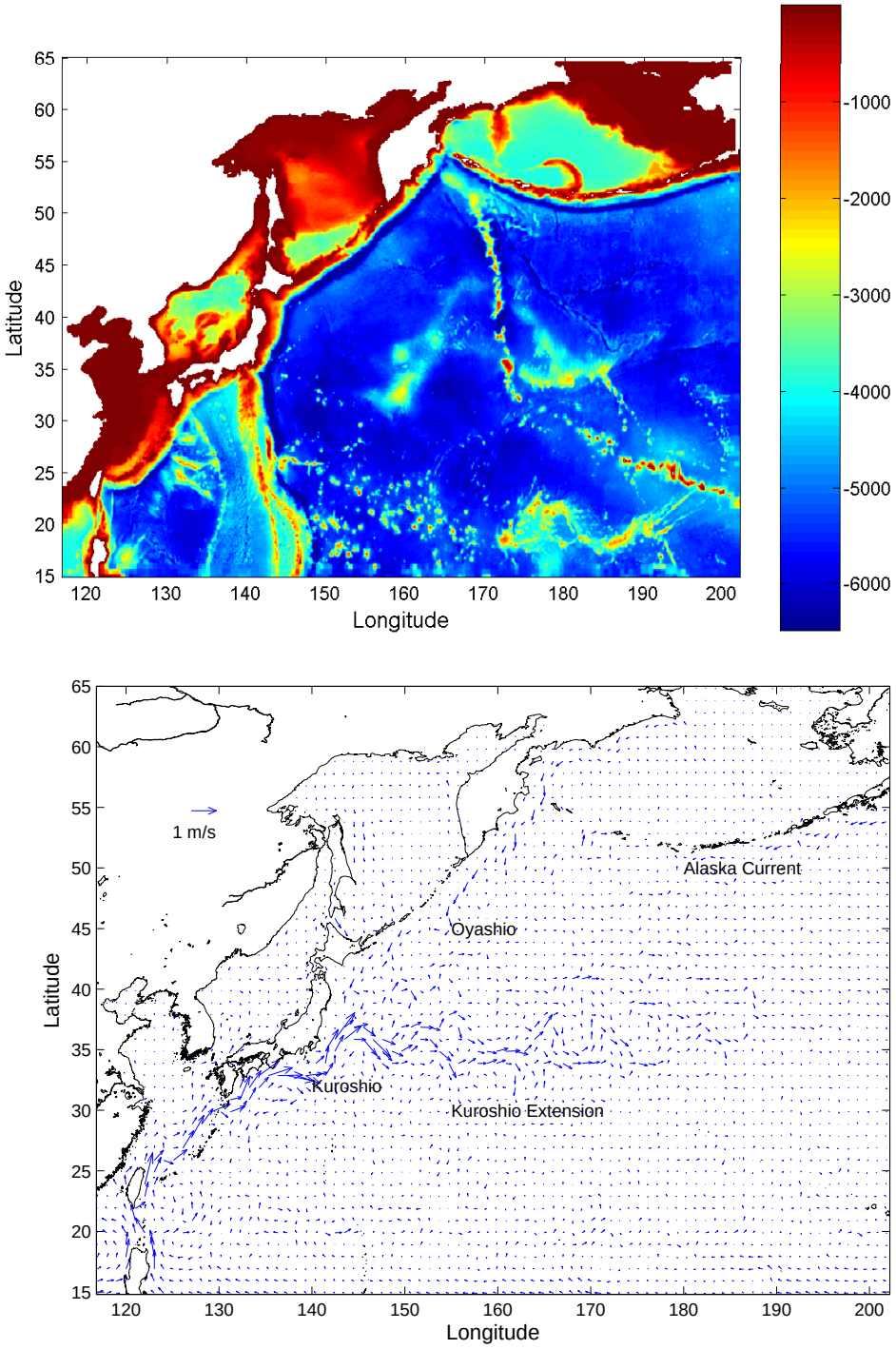

Figure 1: Water depths (m) over the model domain and average water circulation in March 2011, as an example, obtained with FORA model.

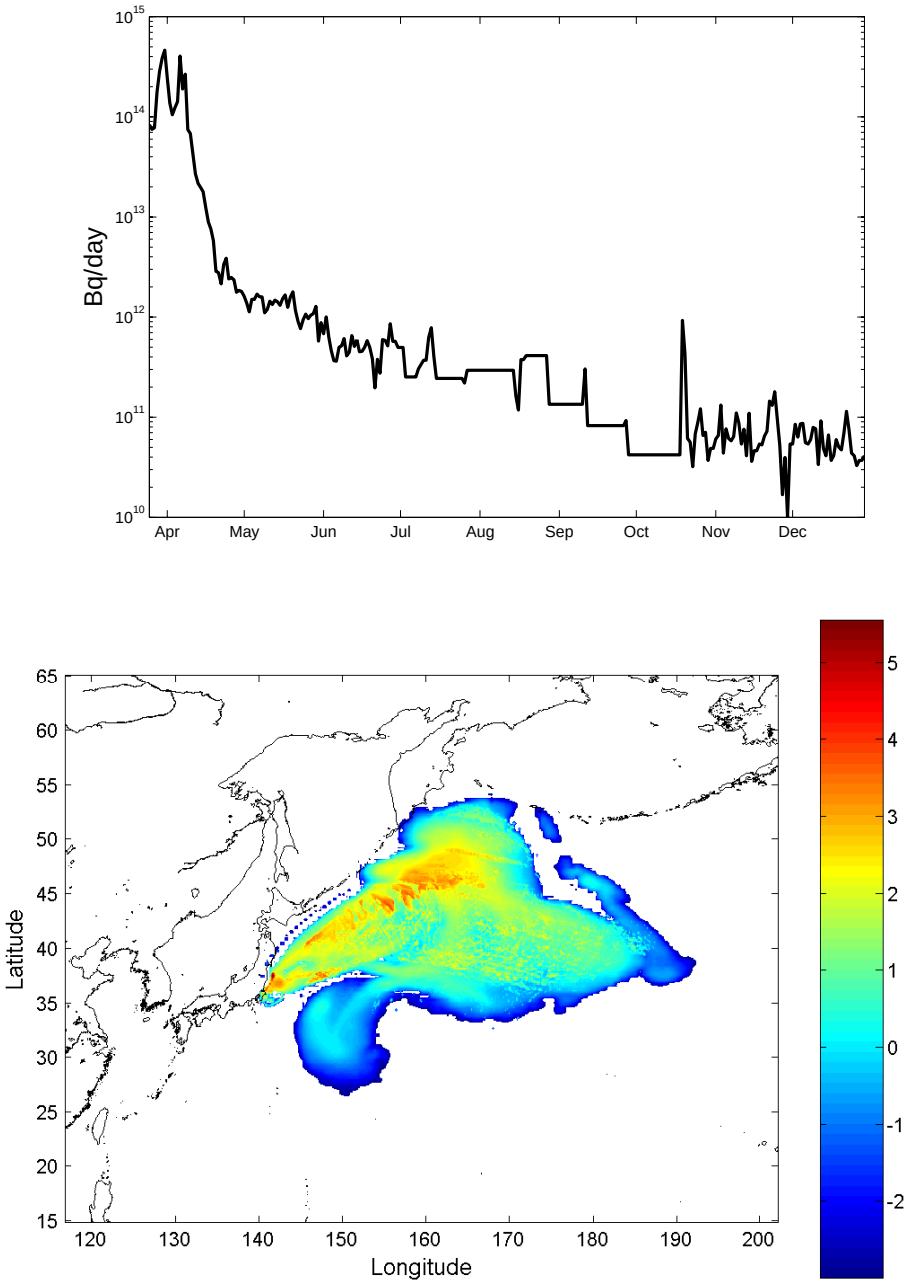

Figure 2: Top: Direct releases from FDNPP into the Pacific Ocean. Bottom: Example of atmospheric deposition for Martch 15th, 2011, in Bq/m^2 (logarithmic scale).

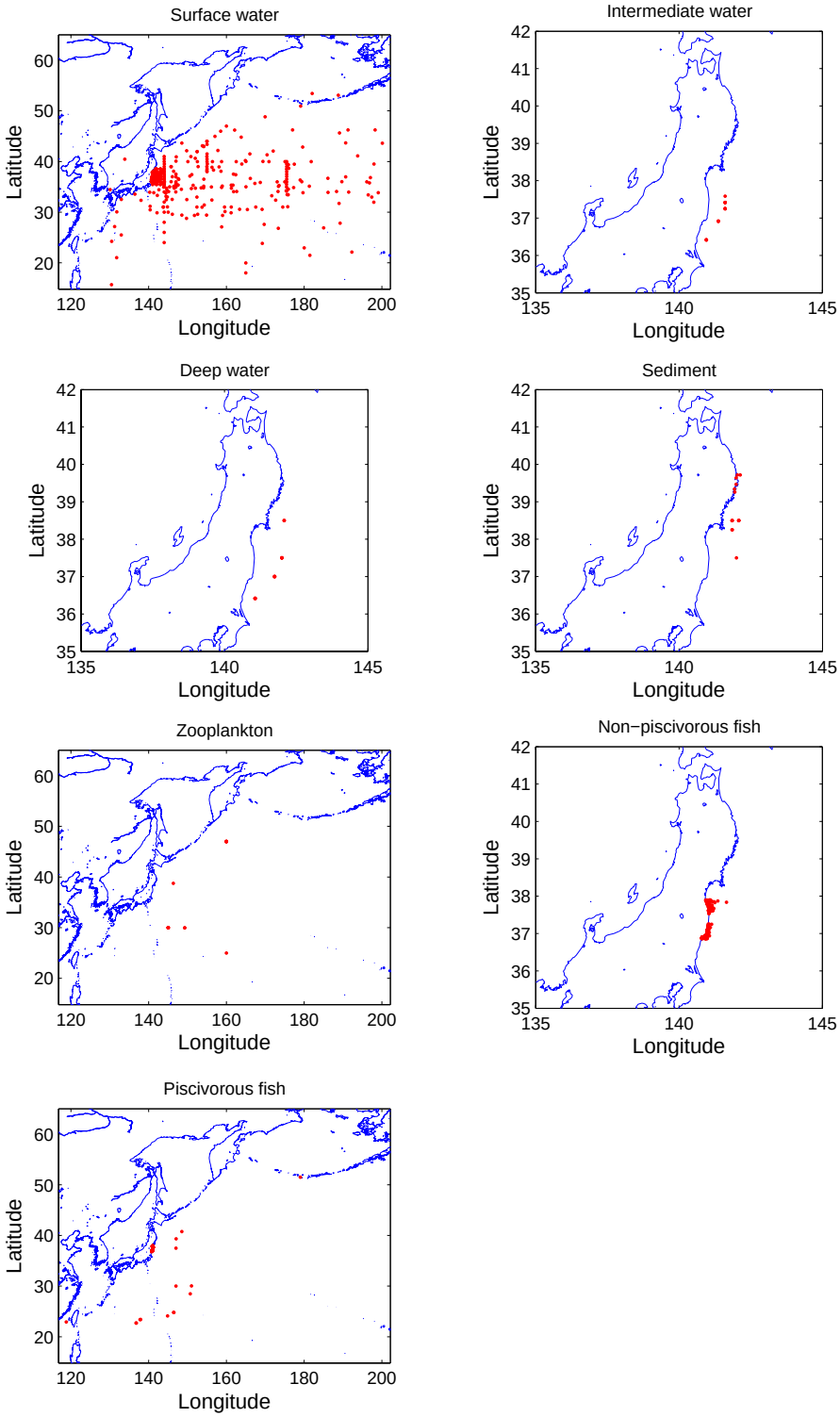

Figure 3: Locations of sampling points for all considered environmental compartments.

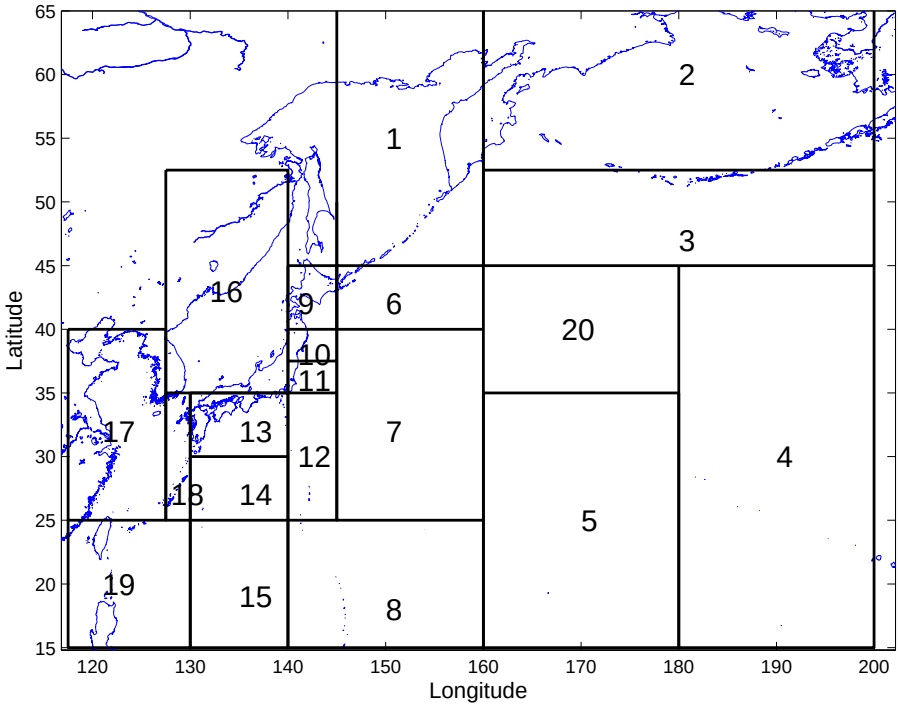

Figure 4: Box division of the Pacific Ocean for model/data comparisons.

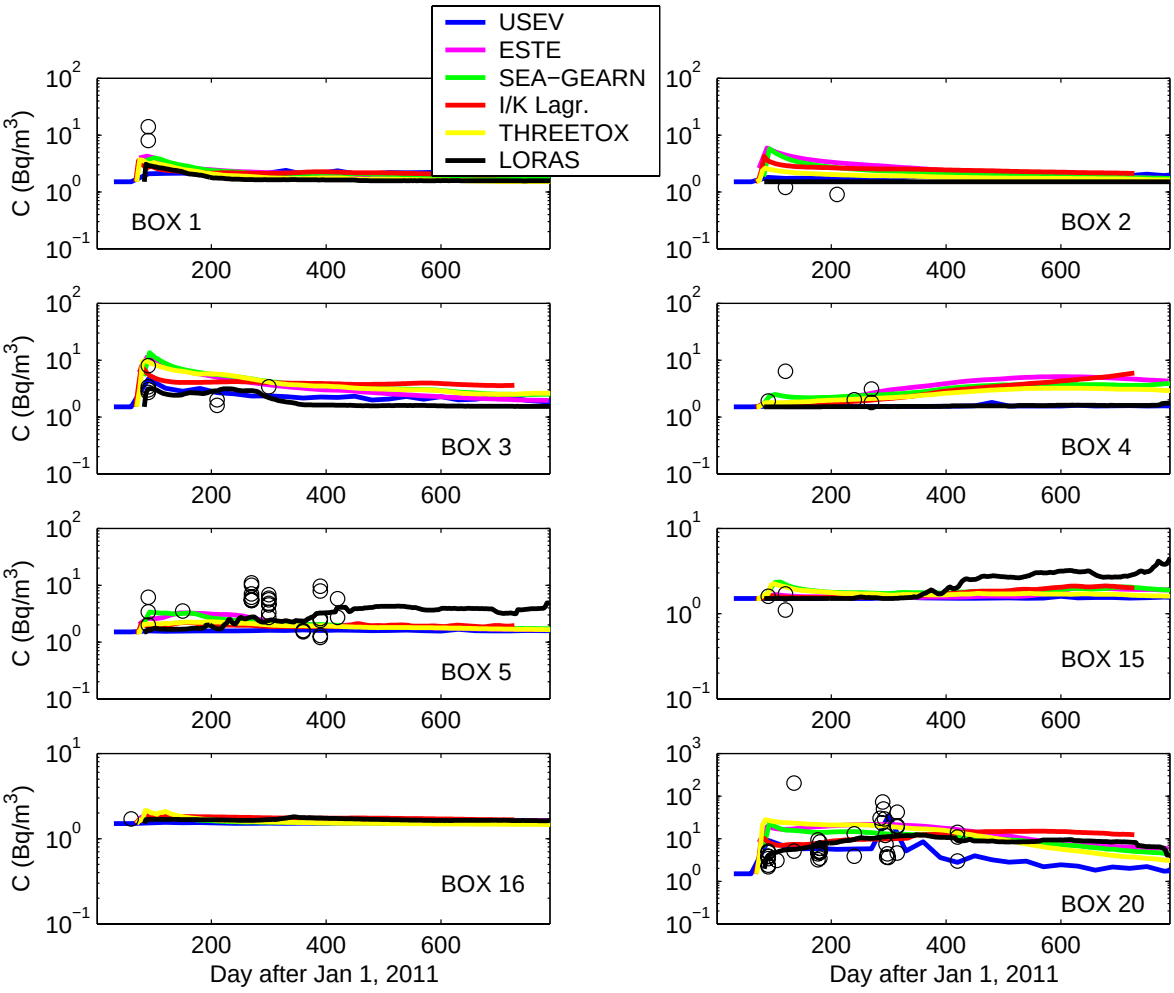

Figure 5: Model predictions and measurements of ^{137}Cs concentrations in surface water for some boxes in the Pacific.

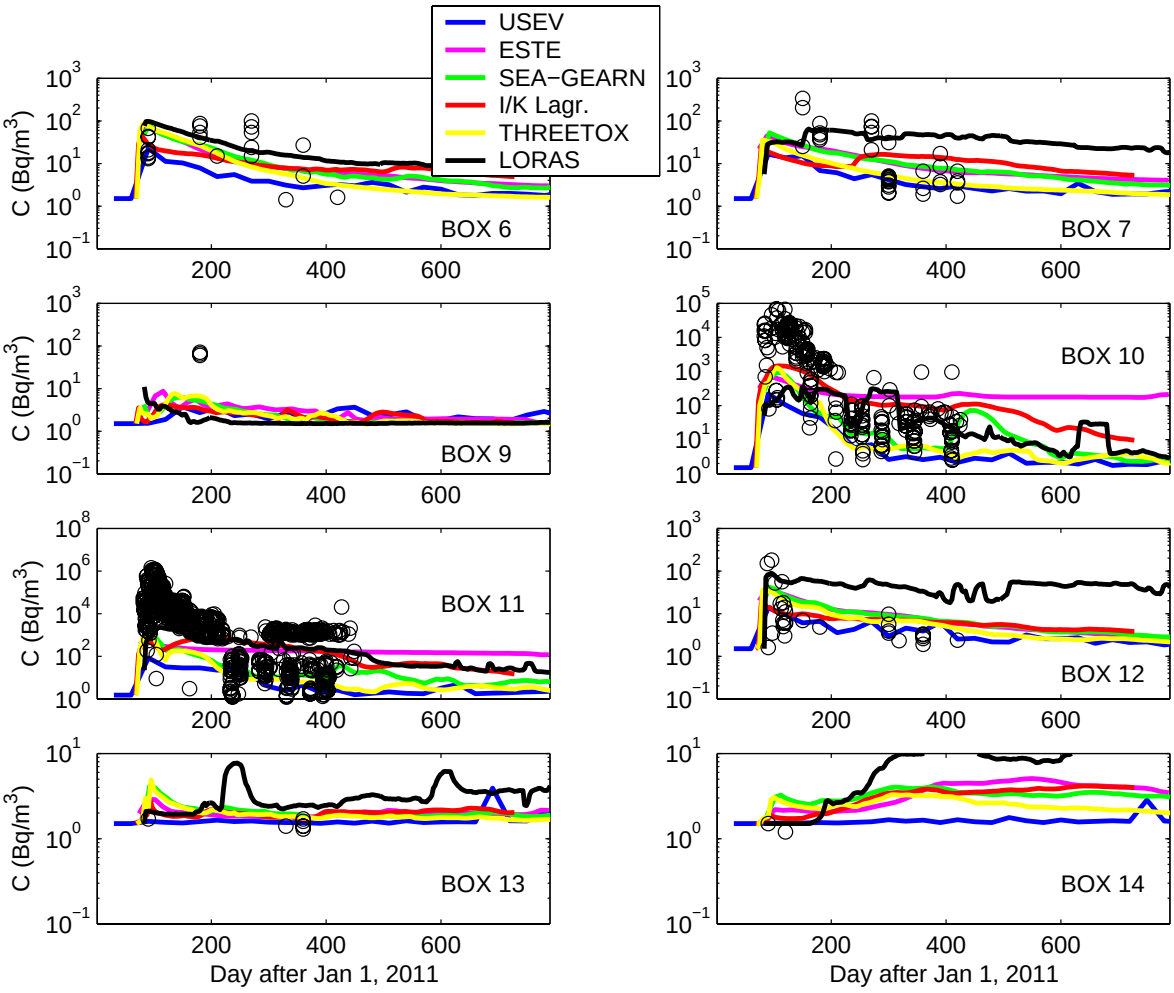

Figure 6: Model predictions and measurements of ^{137}Cs concentrations in surface water for some boxes in the Pacific.

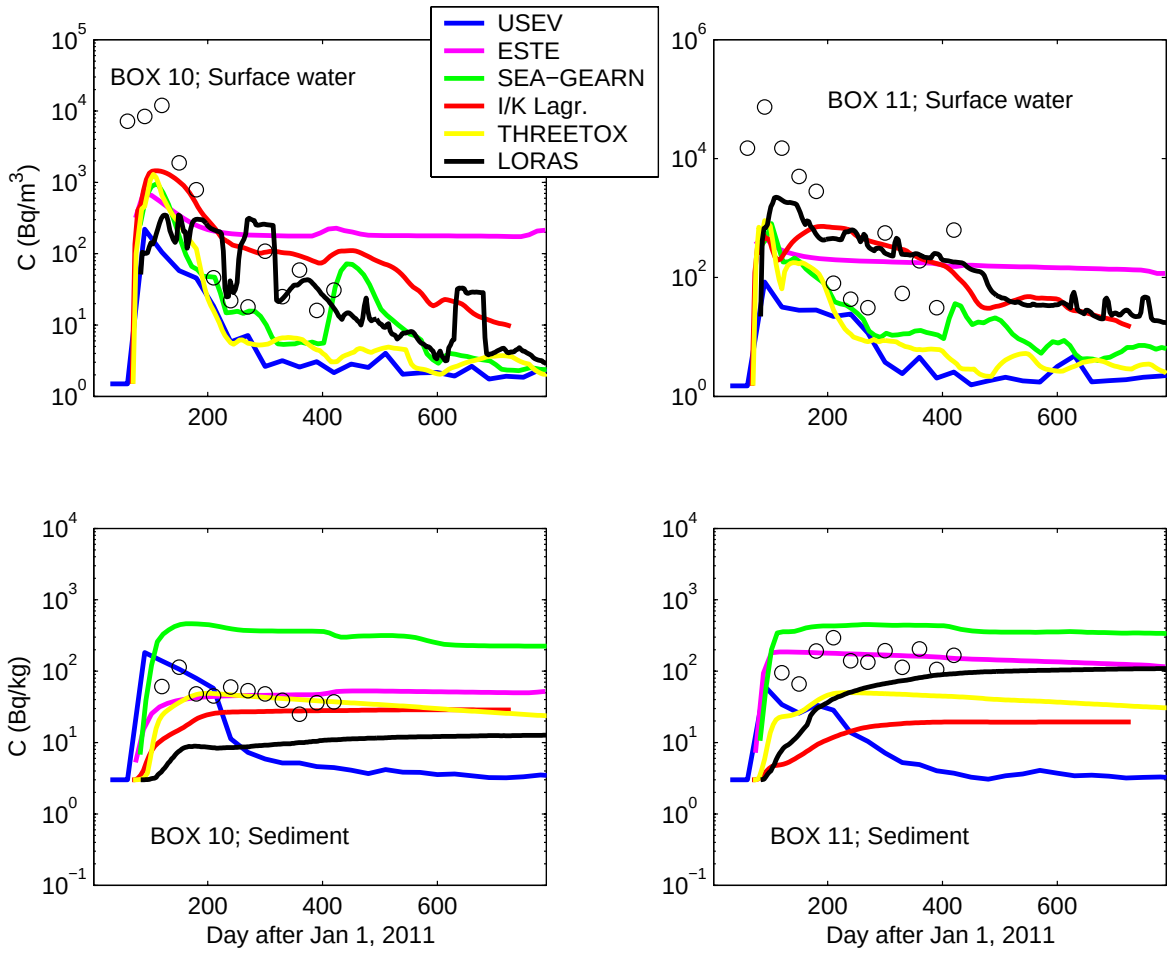

Figure 7: Model predictions and geometric means of ^{137}Cs concentrations measured for each month in boxes 10 and 11, for surface water and sediments. Geometric standard deviations are not drawn because they are too small compared with the vertical scales.

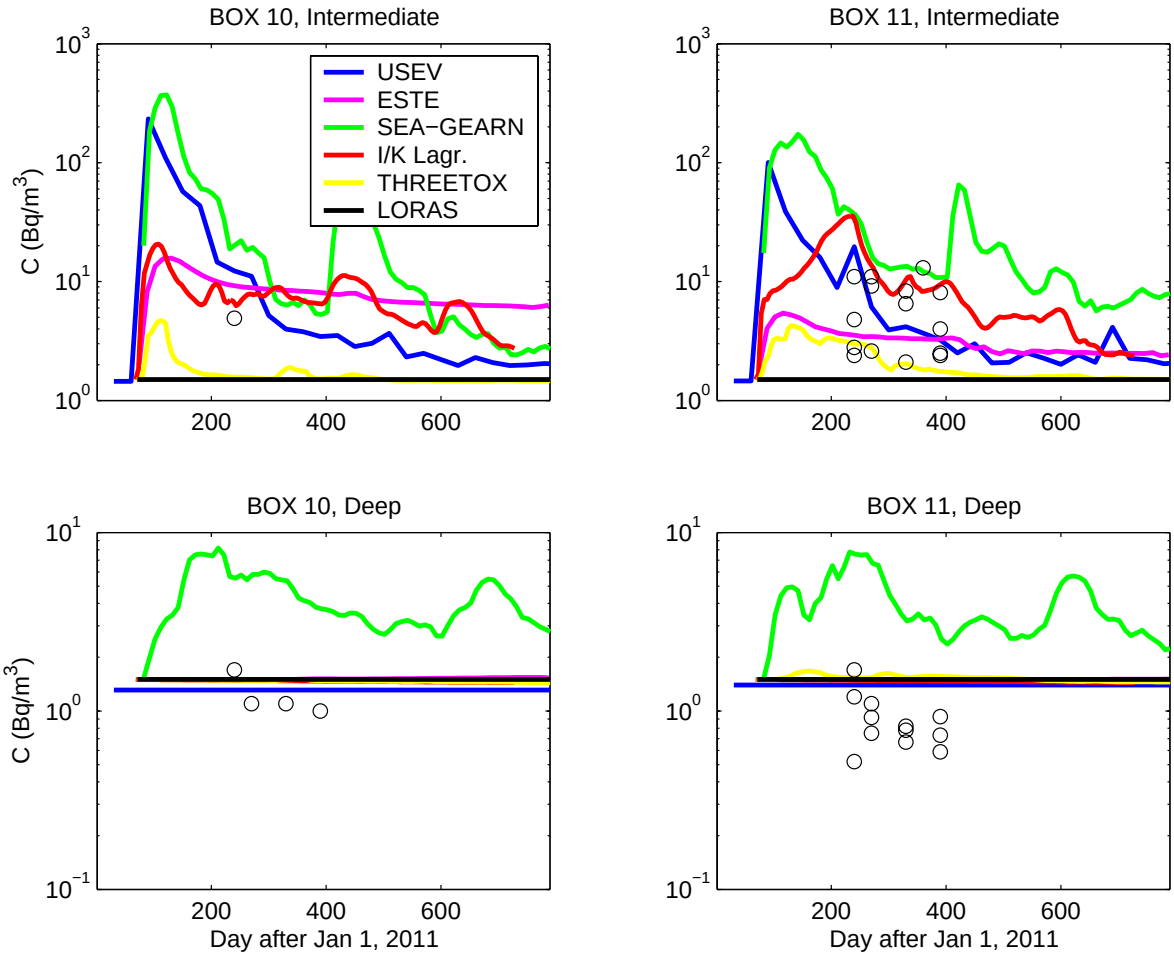

Figure 8: Model predictions and measurements of ^{137}Cs concentrations in intermediate and deep waters for some boxes in the Pacific.

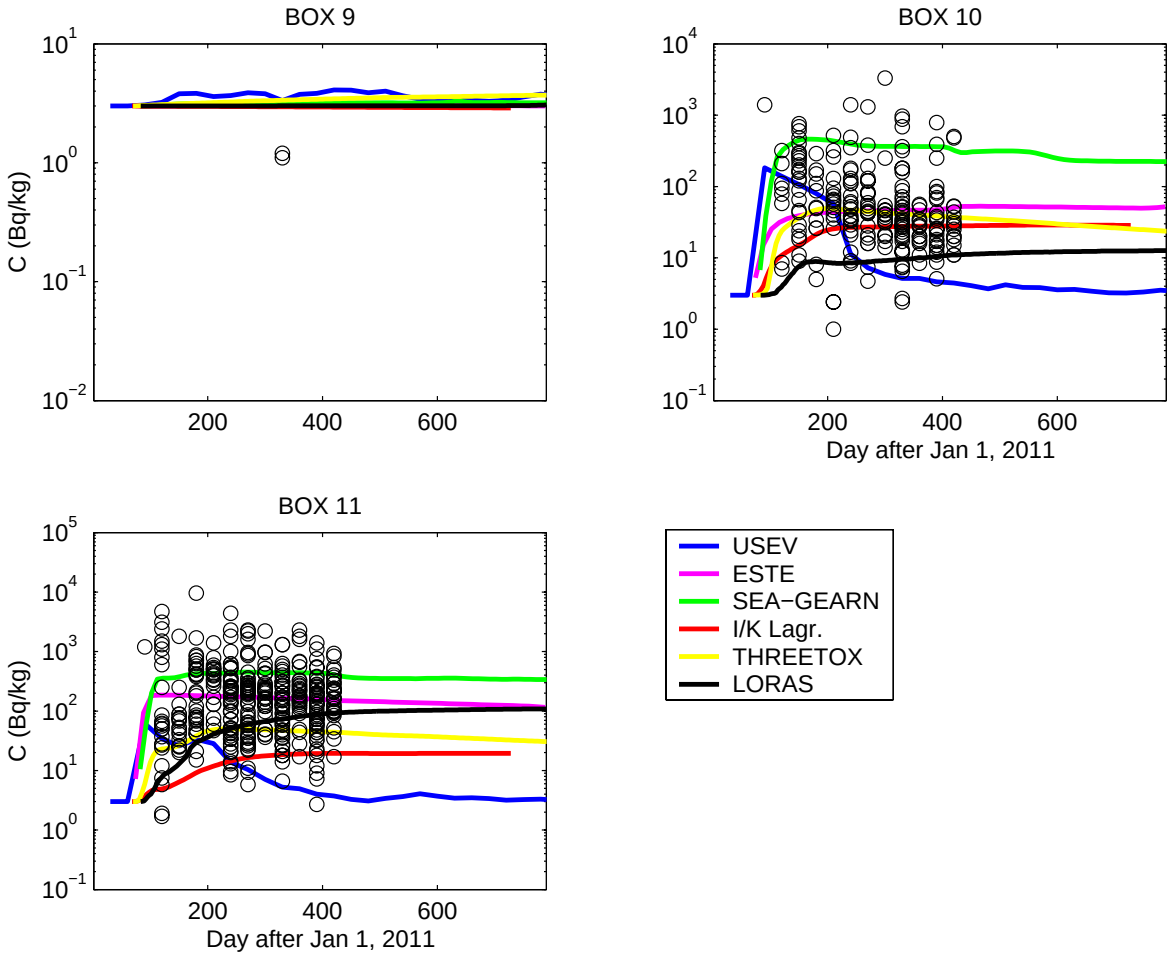

Figure 9: Model predictions and measurements of ^{137}Cs concentrations in bed sediments for some boxes in the Pacific.

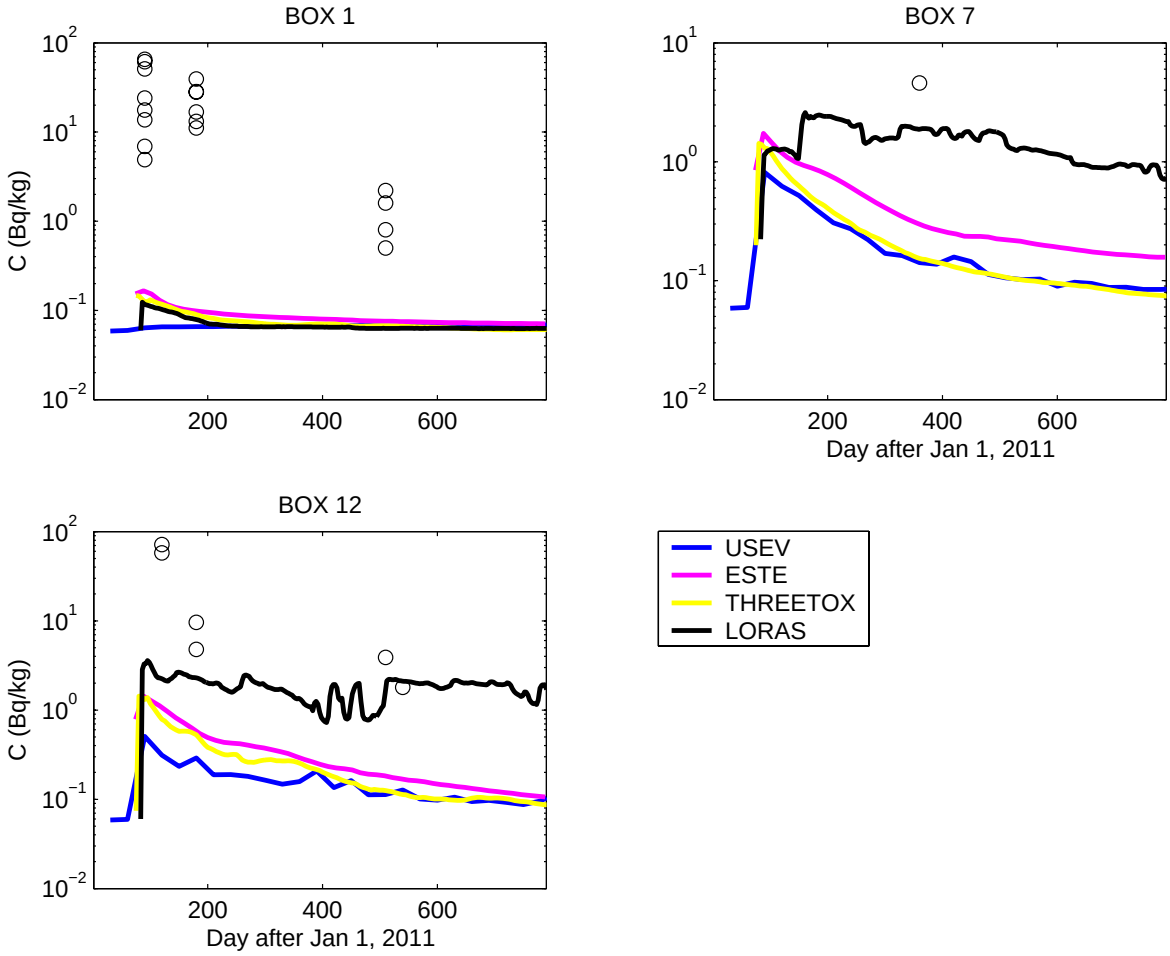

Figure 10: Model predictions and measurements of ^{137}Cs concentrations in zooplankton for some boxes in the Pacific (Bq/kg wet weight).

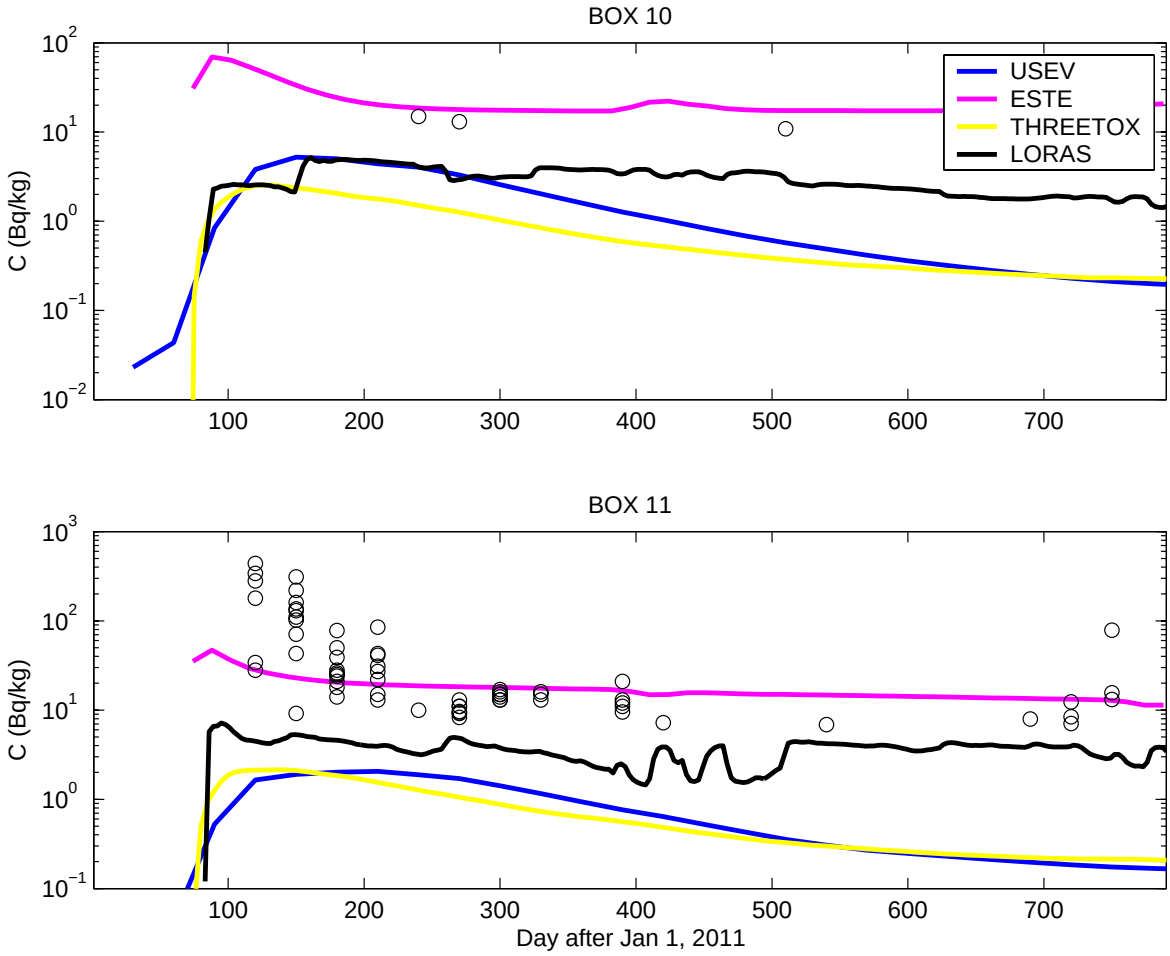

Figure 11: Model predictions and measurements of ^{137}Cs concentrations in non-piscivorous fish (pelagic) for some boxes in the Pacific (Bq/kg wet weight).

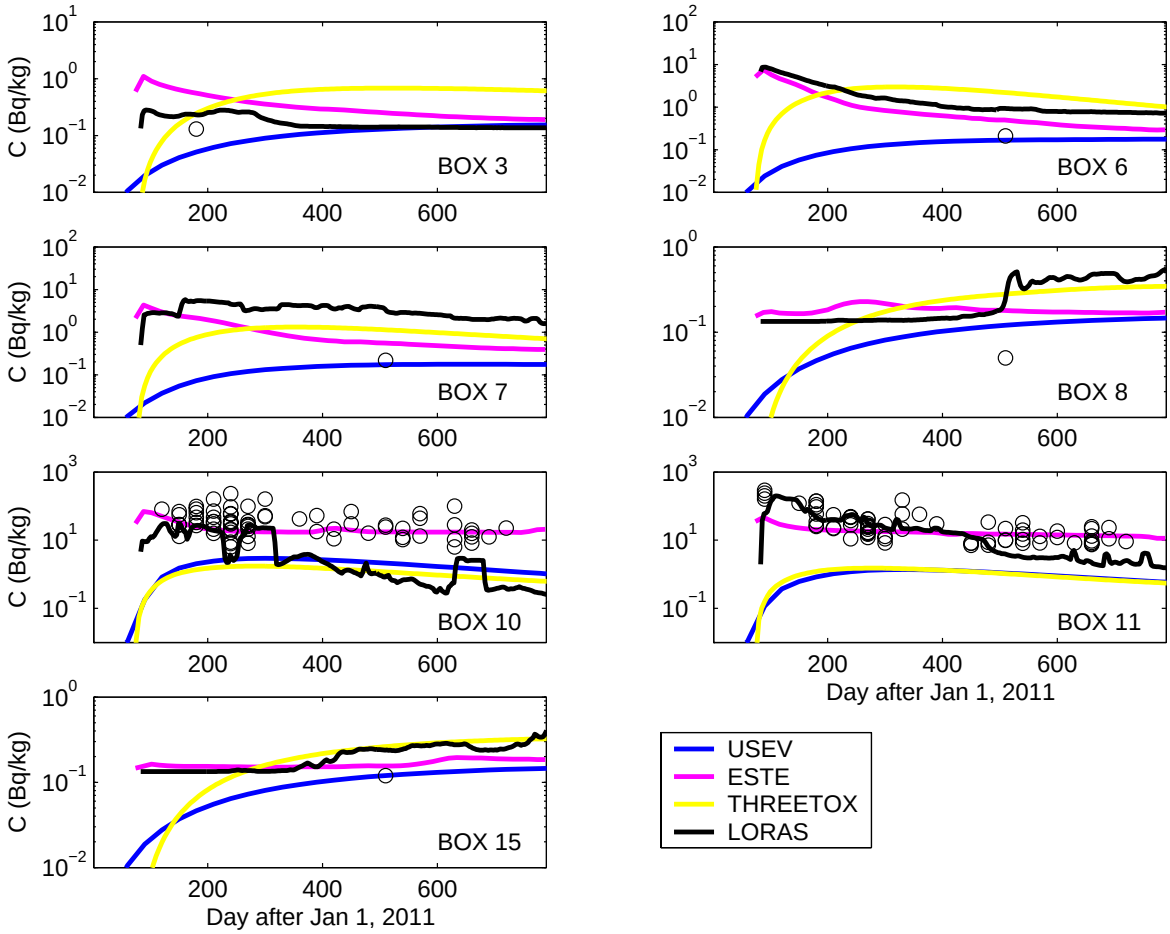

Figure 12: Model predictions and measurements of ^{137}Cs concentrations in piscivorous fish (pelagic) for some boxes in the Pacific (Bq/kg wet weight).

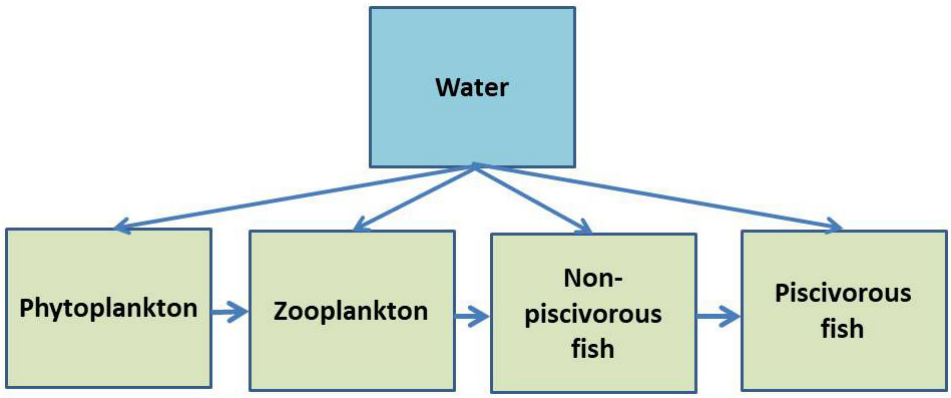

Figure 13: Scheme of radionuclide transfer (arrows) in a dynamic food chain model (from Maderich et al., 2014a).